

# MD/GE - Molecular dynamics simulation and lattice energy of argon

Protocol for the PC 2 lab course by  
**Vincent Kümmerle & Elvis Gnaglo & Julian Brügger**

University of Stuttgart

authors: Vincent Kümmerle, 3712667  
st187541@stud.uni-stuttgart.de

Elvis Gnaglo, 3710504  
st189318@stud.uni-stuttgart.de

Julian Brügger, 3715444  
st190050@stud.uni-stuttgart.de

group number: A05

date of experiment: 10.12.2025

supervisor: Xiangyin Tan

submission date: January 14, 2026

**Abstract:** Molecular Dynamics Simulations (MDS) were used to simulate the sublimation curve and phase transitions of Argon. The onset of the simulated sublimation curve was located 10 K lower, the melting and boiling points  $T_m \approx 77$  K and  $T_b \approx 137$  K deviate due to not enough iterations in the Velocity-Verlet algorithm and approximations made in the used LJ-potential.

The sublimation enthalpy of argon was calculated as  $\Delta H_{\text{sub}} = 8325.640 \frac{\text{J}}{\text{mol}}$ , the lattice energy with experimental values as  $U_{\text{lattice,D}} = -8742.961 \frac{\text{J}}{\text{mol}}$  and the theoretical energy as  $U_{\text{lattice,E}} = -8441.849 \frac{\text{J}}{\text{mol}}$ . The deviation from the theoretical lattice energy was 3.6%, which shows that the LJ-potential provides a good approximated value for the lattice energy of argon.

# Contents

|  |           |
|--|-----------|
| <b>1 Theory</b>                              | <b>1</b>  |
| <b>2 Procedure</b>                           | <b>3</b>  |
| 2.1 Molecular Dynamics Simulations . . . . . | 3         |
| 2.2 Lattice energy of argon . . . . .        | 3         |
| <b>3 Results</b>                             | <b>5</b>  |
| <b>4 Analysis</b>                            | <b>7</b>  |
| 4.1 Molecular Dynamics Simulations . . . . . | 7         |
| 4.1.1 Isochor simulations . . . . .          | 7         |
| 4.1.2 Isobaric simulations . . . . .         | 9         |
| 4.2 Lattice energy of argon . . . . .        | 12        |
| <b>5 Error Discussion</b>                    | <b>14</b> |
| <b>6 Conclusion</b>                          | <b>14</b> |
| <b>7 References</b>                          | <b>15</b> |

## 1 Theory

Molecular dynamics simulations are used to visualize spatial movements of atoms and molecules. For that a numerical algorithm can determine the positions  $r_i$  and momentums  $p_i$  for each particle  $i$ .<sup>[1]</sup> A proven algorithm is the Velocity-Verlet algorithm, which assigns each particle a random starting position and velocity at first before calculating the new positions and velocities a small time step later. That is achieved by calculating the new accelerations using the provided potential, e.g. lennard-Jones potential. So for the computation of particle trajectories in MDS the equation of motion is integrated and then the forces induced by potentials are calculated. To approximate the intermolecular interactions between particles, the Lennard-Jones potential (LJ-potential)  $V_{ij}$  with equation 1 is used.<sup>[1]</sup>

$$V(r_{ij}) = 4\epsilon_0 \left[ \left( \frac{\sigma_0}{r_{ij}} \right)^{12} - \left( \frac{\sigma_0}{r_{ij}} \right)^6 \right], \quad (1)$$

$\sigma_0$  describes the minimum distance,  $r_{ij}$  the distance between particle  $i$  and  $j$  and  $\epsilon_0$  the depth of the potential well at the equilibrium distance  $r_e$ , which can be seen in figure 1. The positive part with a twelfth power-term characterizes the repulsive interactions to the nearest neighbours, whereas the negative part with a sixth power-term characterizes the attractive electrostatic interactions.<sup>[1]</sup>

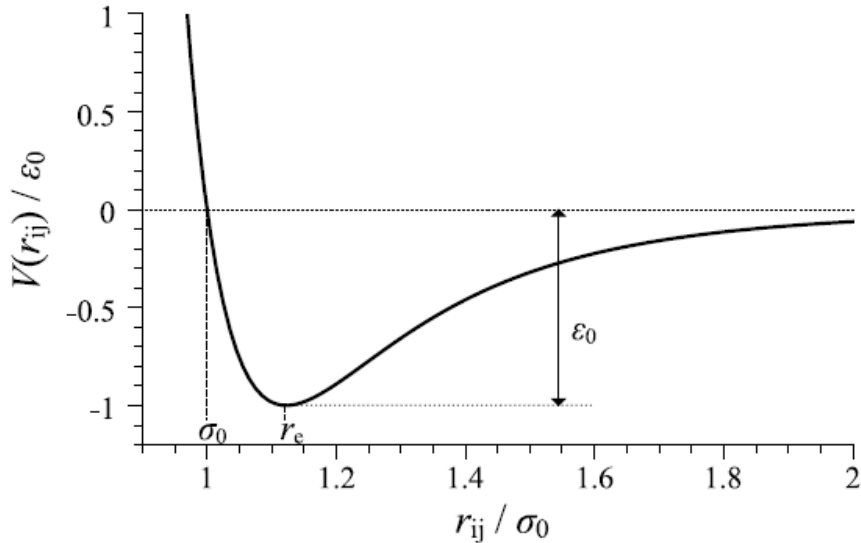


Figure 1: Potential curve of a Lennard-Jones potential  $V_{ij}$  depending on the particle distance  $r_{ij}$ .<sup>[1]</sup>

In MDS reduced properties are used to describe thermodynamical states by defining units and setting the value to 1.0 for shorter calculation times. When using the LJ-potential the fundamental units  $\epsilon_0$ ,  $\sigma_0$  and the mass  $m$  are set to 1.0. In the experiment the reduced units of pressure  $p^*$  and temperature  $T^*$  are used, which can be calculated with equation 2 and 3.

$$T^* = \frac{k_B T}{\varepsilon_0} \quad (2)$$

$$p^* = \frac{p \sigma_0^3}{\varepsilon_0} \quad (3)$$

In an isolated system, where the gaseous and solid phase are in equilibrium and the volume of the gas is much bigger than the volume of the liquid, the Clausius-Clapeyron equation 4 can be used to describe the dependence of the sublimation pressure  $p$  on the temperature  $T$ .

$$\ln p = -\frac{\Delta H_{\text{sub}}}{RT} + C \quad (4)$$

The enthalpy of sublimation  $\Delta H_{\text{sub}}$  can be determined by plotting  $\ln p$  against  $1/T$ . Argon behaves like an ideal gas at 70 K and the internal energy  $\Delta U$  during a phase transition from solid to gaseous is the difference of the corresponding internal energies. Because the translational energy of gaseous argon corresponds to the kinetic theory of gases, the total internal energy of the solid  $U_s$  can be calculated with equation 6.

$$U_s = \frac{5}{2}RT - \Delta H \quad (5)$$

$U_s$  consists of two parts, which are described in equation 5.<sup>[1]</sup>

$$\Delta U_s = U_{\text{lattice,D}} + U_{\text{vib}} \quad (6)$$

The first part corresponds with the potential energy of argon atoms at rest on their lattice planes, whereas the second part is the vibrational energy of the atoms. For the calculation of  $U_{\text{vib}}$ , Debyes theory is used, which states that the crystal is composed as independent vibrating lattice atoms with varying frequencies. For that the equation 7 shows the connection between the vibrational energy and the Debye-temperature  $\Theta_D$ .

$$U_{\text{vib}} = \frac{9}{8}R\Theta_D + 3RTD \left( \frac{\Theta_D}{T} \right) \quad (7)$$

To calculate the theoretical value of the lattice energy, equation 8 can be used, which is derived from the pair potentials  $V_{ij}(r_{ij})$  in the LJ-potential equation 1.

$$U_{\text{lattice,E}}(s) = 2N_A\varepsilon_0 \left[ 12.132 \left( \frac{\sigma_0}{a} \right)^{12} - 14.454 \left( \frac{\sigma_0}{a} \right)^6 \right] \quad (8)$$

$N_A$  is Avogadro's constant and  $a$  the distance between atoms.

## 2 Procedure

### 2.1 Molecular Dynamics Simulations

The three simulations were done using pre-written Python scripts based on the program espresso. The first task showcased the behavior of argon atoms in a given space at constant pressure while steadily increasing the temperature. The simulation visualized the change in particle motion and speed as well as the associated expansion of the system volume. This was done by increasing the number of cooling steps and the interaction potential depth  $\varepsilon_0$  to observe their influence on the system.

The second task studied the behavior of argon during sublimation. This was done with a three core simulation under constant volume and increasing temperature and pressure. Initially, the system was simulated using 100 cycles with 1000 steps. Afterwards it was repeated but the parameters were increased to 200 cycles and 4000 steps. The resulting pressure-temperature dependence obtained from the simulations was then compared with the experimental measurements.

In the third task the temperature dependence of the volume was investigated. For this, three simulations with four cores and progressively increased cooling cycles and cooling steps were carried out. The first simulation used 50 cooling cycles with 100 cooling steps, followed by 10 iteration cycles and 100 iteration steps to show the difference in quality. The second simulation increased the cooling cycles and the number of iteration cycles to 100 and the cooling steps to 1000. In the final simulation, the number of iteration steps was increased to 1000. The results of these simulations were compared to analyze phase transitions and to determine the melting and boiling points of argon.

### 2.2 Lattice energy of argon

The experimental setup was already built prior to the start of the measurements as shown in figure 2.

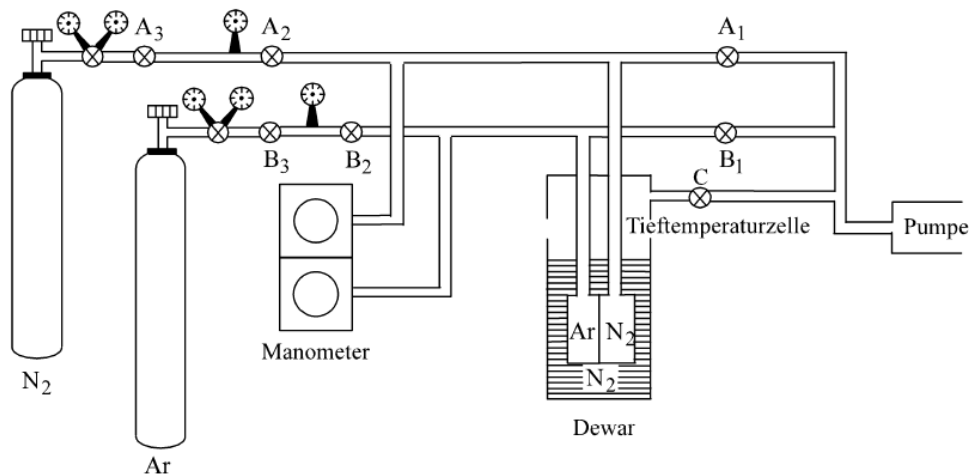


Figure 2: Scheme of the experimental setup with two manometers for measuring the pressure of the argon and nitrogen chamber.<sup>[1]</sup>

The experiment began with the removal of residual gases from the system, which was achieved by flushing the apparatus with nitrogen gas followed by evacuation. The pressure was checked for two minutes to verify the absence of leaks and the vacuum pump was activated. After confirming that the pressure was constant with a correction pressure of 0.6 mbar, the valve for the argon chamber was opened to set a pressure of approximately 250 mbar and cooled to approximately 64 K, leading to a pressure decrease to about 16 mbar. Once 16 mbar argon pressure was reached, the nitrogen chamber was filled to the required level and was cooled to 64 K. After all pressures stabilized, the valves were closed, the Dewar vessel was sealed, and the valve to the vacuum pump was opened. Pumping nitrogen gas from the Dewar reduced the system temperature in the cryogenic cell as much as possible. Under these conditions, the pressure in the argon chamber was approximately 16 mbar and the nitrogen chamber about 144 mbar. After maintaining constant pressure for two minutes, the pump was switched off and the system was allowed to warm up. During the warm-up phase, the pressures in both chambers were noted at intervals of 30 seconds, by reading the manometer display, which showed the pressures in 0.1 bar.

### 3 Results

The measured pressures were first corrected by 0.6 mbar, then converted to bar and after that the pressure of nitrogen was converted to torr with

$$1 \text{ bar} = 750.062 \text{ torr},$$

which lead to the pressure data listed in table 1. Additionally, the temperature was calculated by rearranging the Henning-Otto equation 9 to  $T$  and inserting the measured pressure of nitrogen in torr.

$$\log(p/\text{torr}) = 7.781845 - \frac{341.619 \text{ K}}{\text{T}} - 0.0062649 \frac{\text{T}}{\text{K}} \quad (9)$$

The calculated values of the temperature in the cryogenic cell are also listed in Table 1.

Table 1: Listed are the measured and transformed pressures of argon and nitrogen as well as the calculated temperature of the system.

| $t$ [s] | $p_{\text{Ar}}$ [bar] | $p_{\text{N}_2}$ [bar] | $p_{\text{N}_2}$ [torr] | $T$ [K] |
|---------|-----------------------|------------------------|-------------------------|---------|
| 0       | 0.0154                | 0.1444                 | 108.3090                | 63.8906 |
| 30      | 0.0176                | 0.1500                 | 112.5093                | 64.1048 |
| 60      | 0.0176                | 0.1496                 | 112.2093                | 64.0897 |
| 90      | 0.0181                | 0.1532                 | 114.9095                | 64.2243 |
| 120     | 0.0222                | 0.1696                 | 127.2105                | 64.8069 |
| 150     | 0.0246                | 0.1834                 | 137.5614                | 65.2629 |
| 180     | 0.0268                | 0.1939                 | 145.4370                | 65.5917 |
| 210     | 0.0287                | 0.2039                 | 152.9376                | 65.8918 |
| 240     | 0.0306                | 0.2156                 | 161.7134                | 66.2282 |
| 270     | 0.0333                | 0.2283                 | 171.2392                | 66.5773 |
| 300     | 0.0346                | 0.2413                 | 180.9900                | 66.9189 |
| 330     | 0.0385                | 0.2549                 | 191.1908                | 67.2609 |
| 360     | 0.0417                | 0.2694                 | 202.0667                | 67.6098 |
| 390     | 0.0448                | 0.2844                 | 213.3176                | 67.9554 |
| 420     | 0.0481                | 0.2996                 | 224.7186                | 68.2912 |
| 450     | 0.0519                | 0.3171                 | 237.8447                | 68.6614 |
| 480     | 0.0565                | 0.3337                 | 250.2957                | 68.9980 |
| 510     | 0.0604                | 0.3522                 | 264.1718                | 69.3578 |
| 540     | 0.0648                | 0.3706                 | 277.9730                | 69.7012 |
| 570     | 0.0692                | 0.3890                 | 291.7741                | 70.0315 |
| 600     | 0.0743                | 0.4091                 | 306.8504                | 70.3785 |
| 630     | 0.0798                | 0.4293                 | 322.0016                | 70.7141 |
| 660     | 0.0848                | 0.4489                 | 336.7028                | 71.0281 |
| 690     | 0.0894                | 0.4694                 | 352.0791                | 71.3452 |

| $t$ [s] | $p_{\text{Ar}}$ [bar] | $p_{\text{N}_2}$ [bar] | $p_{\text{N}_2}$ [torr] | $T$ [K] |
|---------|-----------------------|------------------------|-------------------------|---------|
| 720     | 0.0957                | 0.4907                 | 368.0554                | 71.6635 |
| 750     | 0.1014                | 0.5137                 | 385.3068                | 71.9954 |
| 780     | 0.1077                | 0.5357                 | 401.8082                | 72.3022 |
| 810     | 0.1146                | 0.5620                 | 421.5348                | 72.6564 |
| 840     | 0.1213                | 0.5823                 | 436.7611                | 72.9211 |
| 870     | 0.1283                | 0.6050                 | 453.7875                | 73.2088 |
| 900     | 0.1355                | 0.6297                 | 472.3140                | 73.5125 |
| 930     | 0.1413                | 0.6525                 | 489.4155                | 73.7849 |
| 960     | 0.1497                | 0.6774                 | 508.0920                | 74.0741 |
| 990     | 0.1570                | 0.7031                 | 527.3686                | 74.3642 |
| 1020    | 0.1653                | 0.7279                 | 545.9701                | 74.6365 |
| 1050    | 0.1727                | 0.7530                 | 564.7967                | 74.9050 |
| 1080    | 0.1813                | 0.7783                 | 583.7733                | 75.1687 |
| 1110    | 0.1897                | 0.8041                 | 603.1249                | 75.4311 |
| 1140    | 0.1907                | 0.8300                 | 622.5515                | 75.6881 |
| 1170    | 0.2060                | 0.8552                 | 641.4530                | 75.9324 |
| 1200    | 0.2147                | 0.8805                 | 660.4296                | 76.1722 |
| 1230    | 0.2241                | 0.9059                 | 679.4812                | 76.4078 |
| 1260    | 0.2340                | 0.9361                 | 702.1330                | 76.6814 |
| 1290    | 0.2432                | 0.9622                 | 721.7097                | 76.9126 |
| 1320    | 0.2522                | 0.9895                 | 742.1863                | 77.1494 |
| 1350    | 0.2615                | 1.0179                 | 763.4881                | 77.3906 |

## 4 Analysis

### 4.1 Molecular Dynamics Simulations

#### 4.1.1 Isochor simulations

The temperatures and pressures calculated in the simulations of the second task are reported in reduced units and shown in Figure 3.



Figure 3: The reduced temperature is plotted against the reduced pressure for 100 cycles and 1000 steps (T2p1, blue) and for 200 cycles and 4000 steps (T2p2, red).

Both simulations show a very low incline before the sublimation, a steep slope while the sublimation and a transition into a linear increase of the pressure after the sublimation has ended. By increasing the number of iteration steps and the number of iterations per temperature from the first simulation T2p1 to the second T2p2, the begin of the big increase in pressure shifts to a higher temperature, while both curves lead to the same value of pressure, from which on they show the same linear increase. To compare the simulation results to the experimental results, the values of the reduced temperature and pressure are converted from reduced units into Kelvin and Pascal by rearranging equations 2 and 3 to the temperature and pressure:

$$T = \frac{T^* \varepsilon_0}{k_B} \quad (10)$$

$$p = \frac{p^* \varepsilon_0}{\sigma_0^3} \quad (11)$$

For Argon the best values, which were determined from other properties of the gas, are  $\varepsilon_0 = 1.643 \times 10^{-21}$  J and  $\sigma_0 = 3.41 \times 10^{-10}$  m.<sup>[2]</sup> By inserting these values in equation 10 and 11, the values of  $T$  and  $p$  are calculated. Then the experimental data values of  $p$  from Table 1 are converted from bar to pascal with

$$1 \text{ bar} = 1 \times 10^5 \text{ Pa.}$$

All converted pressure values of the simulation and experiment are plotted against the temperature in Figure 4.

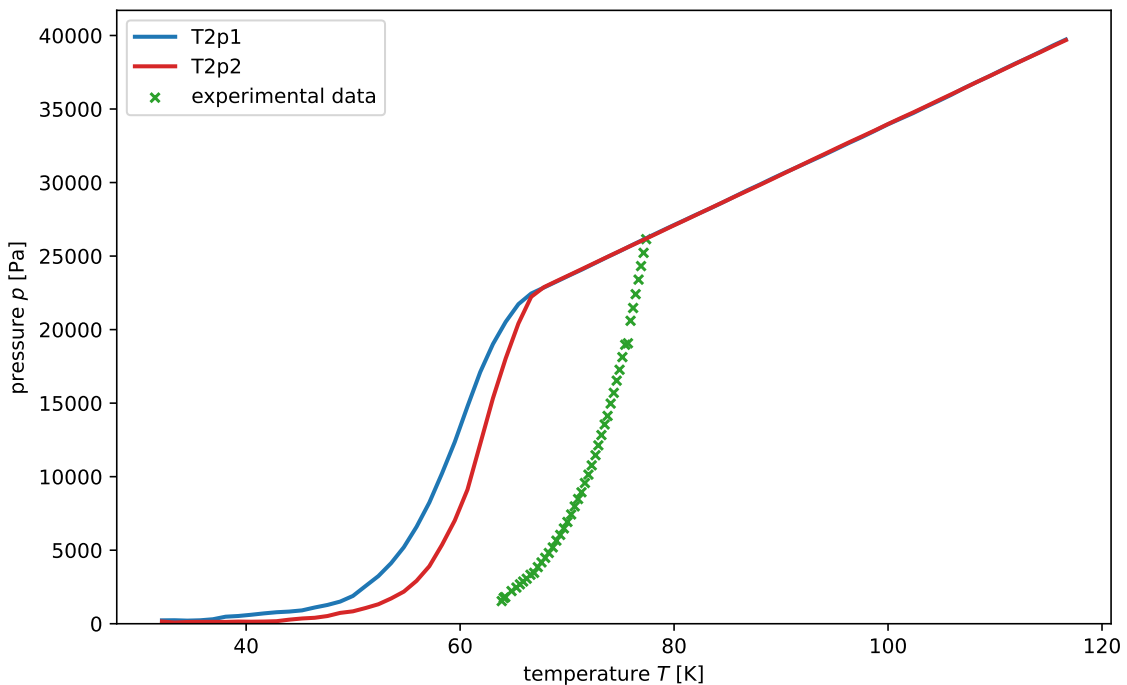


Figure 4: The converted temperature is plotted against the converted pressure from the short simulation (T2p1, blue), long simulation (T2p2, red) and the experimental values (green).

Figure 4 shows that the sublimation curve of the longer simulation with more iteration steps and cycles is closer to the experimental data than the shorter simulation. But still, the experimental sublimation curve is located around 10 K higher, which can be caused by the approximation of the interactions, which are made in the Lennard-Jones potential. Furthermore, it can be concluded that a higher computation time with more iteration steps and cycles in the Velocity-Verlet algorithm would be necessary to fit the simulation values to the experimental values.

#### 4.1.2 Isobaric simulations

As in the previous section discussed, the simulation-results were given in reduced temperature values that were transformed into temperature values in Kelvin to plot figure 5

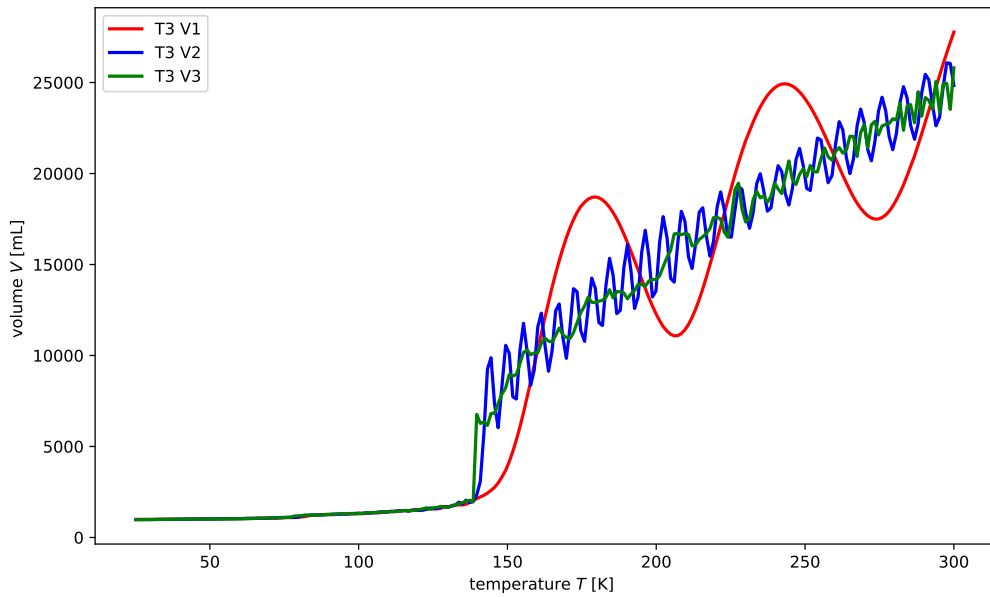


Figure 5: The volume plotted against the temperature for the three simulations.

Curve T3V1 corresponds to the simulation performed with 50 cooling cycles, 100 cooling steps, 10 cycles, and 100 steps. Curve T3V2 represents the simulation using 100 cooling cycles, 1000 cooling steps, 100 cycles, and 100 steps, while plot T3V3 shows the simulation with identical parameters to the second case but with the number of steps increased to 1000. A comparison of the three simulations reveals a clear reduction in the oscillation of the volume as the number of cycles and steps increases. Simulations with a lower numerical resolution do not sufficiently sample the available microstates, which results in oscillations between configurations that are gas-like and configurations that are liquid-like. By increasing the number of steps, these fluctuations are significantly reduced, leading to a smoother volume-temperature curve and minimal background noise, as observed in plot T3V3. Higher step and cycle counts also allow the phase transitions to be identified more distinctly. This is evident from the increase in volume in plot T3V3, which is much more abrupt than in curve T3V1 and T3V2. To determine the melting and boiling points, the regions of rapid volume increase were analyzed in greater detail. These characteristic changes are highlighted in figures 6 and 7, where the volume increase is shown in the temperature intervals around the melting and boiling point.



Figure 6: The volume plotted against the temperature for the three simulations between 70 K and 90 K.

In figure 6, the increase in volume is associated with the onset of melting. For the simulation T3V3, this transition begins at approximately 77 K, whereas for T3V2 and T3V1 it occurs at around 79 K, although the melting point in T3V1 is less clearly defined due to stronger variation in the volume increase. In all cases, the steep rise in volume transitions back into the approximately linear behavior observed at lower temperatures once a temperature of about 82 K is reached. The melting temperatures obtained from the simulations deviate from the literature value for argon, which is approximately 84 K.<sup>[3]</sup> This discrepancy can be attributed to all the approximations that were made during the simulation.

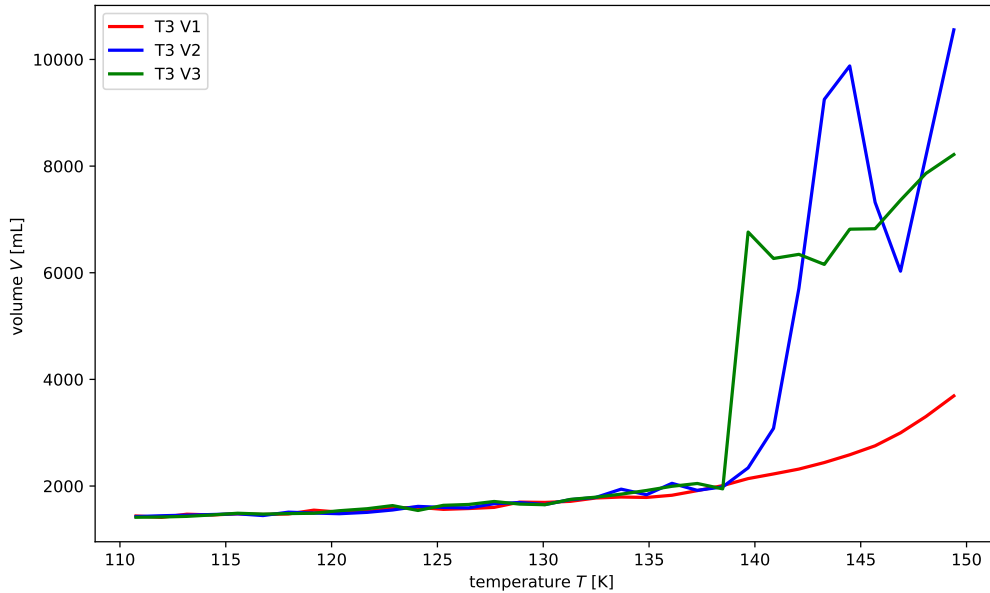


Figure 7: The volume plotted against the temperature for the three simulations between 110 K and 150 K.

When examining figure 7, an increase in volume is observed for the simulations T3V2 and T3V3, while no comparable increase is present in T3V1. This behavior arises from the increased number of cycles and steps used in T3V2 and T3V3, which leads to a more accurate representation of the phase transition. This interpretation is further supported by the fact, that the volume increase in T3V3 is sharper than in T3V2. The observed incline occurs at approximately 137 K, which deviates significantly from the literature boiling point of argon at 87 K.<sup>[3]</sup> As with the melting point, this discrepancy can be attributed to simplifications and approximations inherent to the simulation model. In this case, the simulated boiling point is 50 K higher than the experimental value, which could be explained by the overestimation of interatomic interactions that stabilize the condensed phase.

## 4.2 Lattice energy of argon

In order to calculate the lattice energy of argon, the measured sublimation enthalpy must first be calculated. The sublimation enthalpy can be determined by plotting the natural logarithm of the pressure of argon in bar from table 1 against  $\frac{1}{T}$ . Figure 8 shows the plotted data.

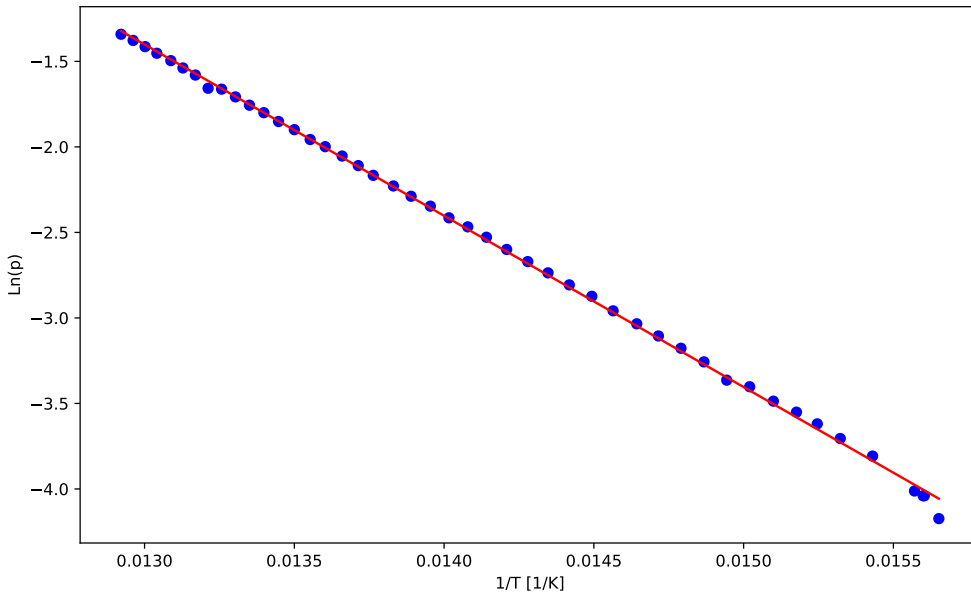


Figure 8: Plot of the logarithm of the pressure of argon in bar against  $\frac{1}{T}$ .

The resulting fit shows a straight line with the function  $y = m \cdot x + b$  with slope  $m = -1001.4 \text{ K}$  and  $b = 11.616$ . By rearranging the Clausius-Clapeyron equation 4 it is possible to calculate the sublimation enthalpy. Using python the error of the slope was calculated  $\delta m = \pm 4.3562 \text{ K}$

$$\Delta H_{\text{sub}} = m \cdot R,$$

The sublimation enthalpy of argon can be calculated as  $8325.640 \frac{\text{J}}{\text{mol}}$ .

By using equation 5 the inner energy of argon can now be calculated.

$$\begin{aligned} U_s &= \frac{5}{2}RT - \Delta H_{\text{sub}} \\ &= \frac{5}{2} \cdot 8.314 \frac{\text{J}}{\text{mol} \cdot \text{K}} \cdot 70 \text{ K} - 8325.640 \frac{\text{J}}{\text{mol}} \\ &= -6870.69 \frac{\text{J}}{\text{mol}} \end{aligned}$$

As equation 6 shows, the lattice energy can be calculated with the internal energy and the vibrational energy. Therefore the vibrational energy has to be calculated, which can be done by using equation 7. The Debye temperature  $\Theta_D = 85\text{ K}$  and the Debye funktion  $D\left(\frac{\Theta}{T}\right) = 0.617$  at  $70\text{ K}$  are given, which means the vibrational energy can be calculated as

$$\begin{aligned} U_{\text{vib}} &= \frac{9}{8}R\Theta_D + 3RTD\left(\frac{\Theta_D}{T}\right) \\ &= \frac{9}{8} \cdot 8.314 \frac{\text{J}}{\text{mol} \cdot \text{K}} \cdot 85\text{ K} + 3 \cdot 8.314 \frac{\text{J}}{\text{mol} \cdot \text{K}} \cdot 70\text{ K} \cdot 0.617 \\ &= 1872.271 \frac{\text{J}}{\text{mol}} \end{aligned}$$

The lattice energy can now be calculated by rearranging equation 6.

$$\begin{aligned} U_{\text{lattice,D}} &= U_s - U_{\text{vib}} \\ &= -6870.69 \frac{\text{J}}{\text{mol}} - 1872.271 \frac{\text{J}}{\text{mol}} \\ &= -8742.961 \frac{\text{J}}{\text{mol}} \end{aligned}$$

The uncertainty of the slope directly affects the uncertainty of the lattice energy which can then be written as  $U_{\text{lattice,D}} = -(8742.961 \pm 4.3562) \frac{\text{J}}{\text{mol}}$ . An alternative method of calculating the lattice energy is by using equation 8. To do this, the minimal distance  $a$  between atoms has to be calculated by using the equation for a face-centered cubic lattice and the lattice constant of argon which is given as  $5.43 \times 10^{-10}\text{ m}$ .

$$\begin{aligned} a &= \frac{1}{\sqrt{2}} \cdot 5.43 \times 10^{-10}\text{ m} \\ &= 3.84 \times 10^{-10}\text{ m} \end{aligned}$$

With  $\sigma_0$  for argon given as  $3.41 \times 10^{-10}\text{ m}$  and  $\epsilon_0$  from the lennard-jones potential given as  $1.643 \times 10^{-21}\text{ J}$  the lattice energy can now be calculated.<sup>[2]</sup>

$$\begin{aligned} U_{\text{lattice,E}}(s) &= 2N_A\epsilon_0 \left[ 12.132 \left( \frac{\sigma_0}{a} \right)^{12} - 14.454 \left( \frac{\sigma_0}{a} \right)^6 \right] \\ &= 2 \cdot 6.022 \times 10^{23} \frac{1}{\text{mol}} \cdot 1.643 \times 10^{-21}\text{ J} \\ &\cdot \left[ 12.132 \cdot \left( \frac{3.41 \times 10^{-10}\text{ m}}{3.84 \times 10^{-10}\text{ m}} \right)^{12} - 14.454 \cdot \left( \frac{3.41 \times 10^{-10}\text{ m}}{3.84 \times 10^{-10}\text{ m}} \right)^6 \right] \\ &= -8252.821 \frac{\text{J}}{\text{mol}} \end{aligned}$$

When compared to the theoretically calculated lattice energy, the experimental lattice energy deviates by approximately 5.6%. This deviation can be explained by leaks in the measuring setup due to it not being perfectly isolated.

## 5 Error Discussion

The room for errors in the molecular dynamics simulations was limited because the Python programs were pre-written and only certain values were manually changed. In the experimental part, the pressures are error-affected, because they were taken from the manometer display and noted every 30s manually. That's why the pressure values exhibit measurement inaccuracy and some outliers, which may have been caused by incorrect readings. That could also be the reason for an inaccurate slope in the fitted plot of the natural logarithm against  $\frac{1}{T}$ , which in turn has an effect on the calculations of the sublimation enthalpy, inner energy and lattice energy. Therefore, it can be assumed that all calculated thermodynamical properties are not exakt because of measurement uncertainty of the manometer or incorrect reading of pressure values. Furthermore, the values could be imprecise because the Dewar was manually attached and screwed to the setup, which is why leaks couldn't be prevented entirely and some liquid nitrogen might have passed out of the system.

## 6 Conclusion

The isochor simulation showed a similar sublimation curve as the experimental sublimation curve, but was located around 10 K lower due to not enough iteration steps and cycles in the Velocity-Verlet algorithm and the approximations made in the used LJ-potential.

The three isobaric simulations showed the importance of computational accuracy, as the simulations with more iteration0 steps were much more compareable to real, experimental data. Although the simulation with the most computational accuracy showed a melting point of  $T_m \approx 77$  K and a boiling point of  $T_b \approx 137$  K which states strong deviation to the measured value especially for the boiling point.

In the practical part of the experiment the sublimation enthalpy of argon was determined as  $\Delta H_{\text{sub}} = 8325.640 \frac{\text{J}}{\text{mol}}$ . That made the calculation of the lattice energy  $U_{\text{lattice,D}} = -8742.961 \frac{\text{J}}{\text{mol}}$  possible. To verify the success of the experiment, the lattice energy calculated from the measured data was compared to the lattice energy calculated from the theoretical parameters  $U_{\text{lattice,E}} = -8252.821 \frac{\text{J}}{\text{mol}}$ . The deviation from the theoretical lattice energy was 5.6%, which shows that the LJ-potential provides a good approximated value for the lattice energy of argon.

## 7 References

- [1] H. Dilger, *2025-pc2-script-en*, **2025**.
- [2] J. O. Hirschfelder, C. F. Curtiss, R. B. Bird, *The molecular theory of gases and liquids*, John Wiley & Sons, **1964**.
- [3] Institut für Arbeitsschutz der Deutschen Gesetzlichen Unfallversicherung, Gestis-Databank, Online Databank, <https://gestis.dguv.de/data?name=007180>.